

Exploring the Role of Nanoparticles Incorporated in PES Membranes for Photodegradation of Persistent Pollutants Under Simulated Sunlight

Hussein Mahmoud El-Ghorab^{1*}, Mahmoud Mohamed Abdel Azeem¹, Mohamed Ismail Badawy², Tarek Abdel Shafy Gad Allah², Mahmoud Saad Abdel Wahed², Mahmoud Mohamed Abdelmomen¹

1. Public Works (Sanitary Engineering) Department, Faculty of Engineering, Ain Shams University, Cairo, Egypt. husseinelghorab@eng.asu.edu.eg, mazeem@eng.asu.edu.eg, mahmoud_abdelmomen@eng.asu.edu.eg
2. Water Pollution Research Department, National Research Centre, Giza, Egypt. badawy46@hotmail.com, tareqabelshafy@yahoo.ca, ms.abdel-wahed@nrc.sci.eg

Abstract

Water scarcity is a critical global issue exacerbated by pollution and inefficient water management. Traditional water treatment methods are often insufficient to address complex pollutants. This study investigates the fabrication and performance of photocatalytic membrane (polyethersulfone (PES) membranes incorporated with photocatalytic nanoparticles of titanium dioxide doped with silver) for photodegradation of trace organic compounds (TrOCs) under simulated sunlight irradiation. The membranes were prepared using the non-solvent induced phase separation (NIPS) method and tested their photocatalytic activity in degrading proteins such as bovine serum albumin (BSA), and dyes such as methyl orange (MO), and methylene blue (MB). Results indicated that the incorporation of nanoparticles significantly improved the degradation efficiency of the pollutants, with the highest performance observed in photocatalytic membranes with the highest nanoparticles content. The study demonstrates the potential of photocatalytic membranes for advanced water treatment applications, offering a promising solution for removal of complex pollutants, mitigating water pollution and scarcity.

Keywords: polyethersulfone, photocatalytic membrane, methylene blue, methyle orange.

1. Introduction

Water, a fundamental necessity for life, is becoming an increasingly scarce resource globally. While our planet is composed of 71% water, only 2.5% of that is freshwater, and an even smaller fraction is accessible for human use. This growing scarcity is exacerbated by factors such as population growth, climate change, pollution, and inefficient water management practices. It is imperative to address water scarcity not only to sustain life but also to promote socio-economic development, health, and environmental sustainability ¹.

The scarcity of water has far-reaching implications. It directly affects agriculture, which consumes approximately 70% of global freshwater supplies. In regions experiencing severe water shortages, crop yields dwindle, leading to food insecurity and economic instability. Urban areas are not immune either; many cities face water rationing and potential conflicts over access to water resources. Moreover, the availability of clean water is crucial for public health. Contaminated water sources can lead to the spread of diseases such as cholera and dysentery, impacting millions of lives, particularly in developing countries ¹.

Given the critical nature of water, effective treatment and management are essential. Water treatment processes are designed to remove contaminants and ensure that water is safe for human consumption and other uses. Traditional treatment methods, such as coagulation, sedimentation, filtration, and disinfection, have been effective to some extent. However, the increasing presence of persistent pollutants, such as pharmaceuticals, dyes, and pesticides, requires more advanced and efficient treatment technologies ¹.

Photocatalytic reactors (PRs) offer an efficient solution for removal of trace organic compounds (TrOCs), where PRs utilize advanced oxidation processes to degrade organic pollutants through the excitation of semiconductor photocatalysts (e.g., TiO_2 , ZnO) by UV or visible light, which generates reactive species that oxidize and break down pollutants.² Despite their effectiveness, photocatalytic reactors face challenges in screening photocatalysts during water treatment. The separation of photocatalysts from treated water can be difficult, leading to potential contamination and reduced efficiency. Traditional methods, such as filtration and centrifugation, may not be sufficient to completely remove the photocatalysts, which can affect the quality of the treated water³.

To address these challenges, photocatalytic membranes have emerged as a promising alternative. These membranes combine the advantages of photocatalysis and membrane filtration, allowing for the simultaneous degradation of pollutants and separation of photocatalysts from treated water. Photocatalytic membranes are typically made of porous materials coated with photocatalytic nanoparticles, which can effectively degrade organic pollutants while retaining the catalysts within the membrane structure, eliminating the risk of catalyst contamination in the treated water, and ensuring higher water quality. Lastly, photocatalytic membranes can be easily scaled up for industrial applications, making them a viable solution for large-scale water treatment⁴.

This study aims to fabricate photocatalytic membrane and to consider the activity of a membrane with light in pollutant removal, while concentrating on assessing the effect of the photocatalyst role in pollutant degradation. The choice of membrane material was Polyethersulfone (PES) being a highly efficient material for water filtration membranes due to its excellent chemical resistance, mechanical strength, and thermal stability. PES membranes are widely used in various filtration applications, including microfiltration, ultrafiltration, and nanofiltration, due to their ability to effectively remove contaminants, making PES a very strong candidate when requiring to immobilize nanoparticles within its structure⁵.

The photocatalytic membranes activity was studied for removal of TrOCs in wastewater conditions, where we used proteins of bovine serum albumin (BSA) to mimic wastewater organic content, and a mixture of methyl orange (MO) and methylene blue (MB) dyes were added for assessment of the membrane performance in photocatalytic degradation of TrOCs.

Previous research of polymeric membrane incorporated with photocatalytic nanostructures where successful in removal of MB to percentages reaching up to 75%⁶, and up to 95% for MO⁷. However, these studies don't interpret the effect of wastewater conditions which would be simulated in our work with the BSA incorporation in the model solution, to further study how it would affect the photocatalytic degradation and adsorption for the membranes, while also incorporating recent progressions in extension of the photocatalytic activity to visible light through doping TiO_2 semiconductor with silver nanoparticles⁸.

2. Experimental Methods

2.1. Materials

Commercial-grade Polyethersulfone Ultrason E6020P (molecular weight = 58,000 g/mol and glass transition temperature, $T_g = 225$ °C) served as the membrane material. Dimethyl sulfoxide (DMSO) was utilized as the solvent for preparing the casting dope solutions. The PNPs comprised of TiO_2 doped with silver. For testing the membrane's photocatalytic performance, the model compounds included bovine serum albumin (BSA, molecular weight = 66,500 g/mol), methyl orange (MO, molecular weight = 327.33 g/mol), and methylene blue (MB, molecular weight = 319.85 g/mol). Molecular structures of PES, MB, and MO are shown in Figure 1.

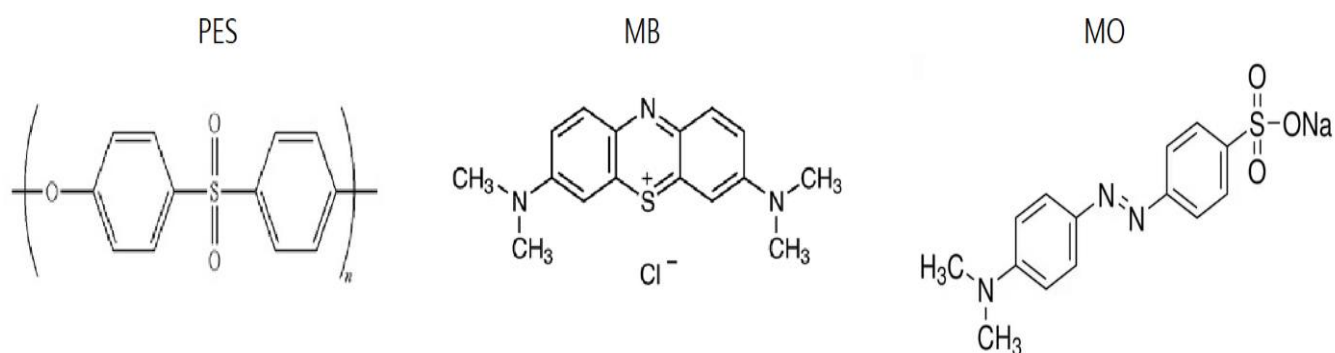


Figure 1: Molecular structure of PES, MB and MO ⁹⁻¹¹

2.2. Membrane Fabrication

Membranes were created using solutions of PES dissolved in DMSO with various amounts of PNP through the non-solvent induced phase separation (NIPS) method. The composition and labeling of PES/PNP membranes are outlined in Table 1.

Table 1: Prepared membranes designations and compositions of casting solutions by weight in mg

Designation	PES	DMSO	PNP
S1	1000	5219	31 (0.5% wt. ratio)
S2	1000	5188	62 (1.0% wt. ratio)
S3	1000	5157	93 (1.5% wt. ratio)

2.3. Membrane Performance

The photocatalytic performance of membranes was tested by a model solution consisting of 250ppm BSA, 10ppm MO and 10ppm MB (pH = 8.1). First, the membrane samples were cut into circle sized samples of diameter 50mm and were fixed in separate petri dishes for each membrane type and then 50 ml of the solution was poured onto it, ensuring contact between solution and membrane sample.

The dishes were fixed in an orbital shaker (WiseShake/Wisd – DAIHANsci) and the samples were gently shaken during the whole period of this setup. The above setup was placed under sunlight irradiation in UVACUBE 400 sunlight simulator (Dr Hönle AG UV Technology, Germany), and solution concentrations were measured every 30 min for a total period of 6 h using a UV/VIS spectrophotometer (Jasco V630), at wavelengths of 290, 465, and 665 nm for BSA, MO, and MB, respectively. Before solar light irradiation, the entire setup was kept in dark conditions for 90 min to attain adsorption equilibrium, and then the solar irradiation took place for the remaining part of the procedure's period ¹².

Prior to the previous experiment, calibration curves were plotted in order to assign the concentrations of the model pollutant constituents precisely. The spectrophotometer was set to the appropriate wavelength for each pollutant and the absorbance was measured and recorded. A graph was plotted for the absorbance values (y-axis) against the known concentrations (x-axis) of the standard solutions. Using best fit linear graphing tool in MS-Excel, a linear regression line was fitted to the data points and the equation of these line were attained ¹³.

3. Results and Discussion

3.1. Calibration Curves

Spectral analysis of all solutions was obtained and plotted properly as shown in Figure 2. The obtained data from that analysis was used to plot the calibration curve for BSA, MO and MB separately as shown in Figure 3, Figure 4 and Figure 5 respectively. The equations acquired from these curves were then used in determining the solution concentration during the photocatalytic activity experiment (See section 3.2)

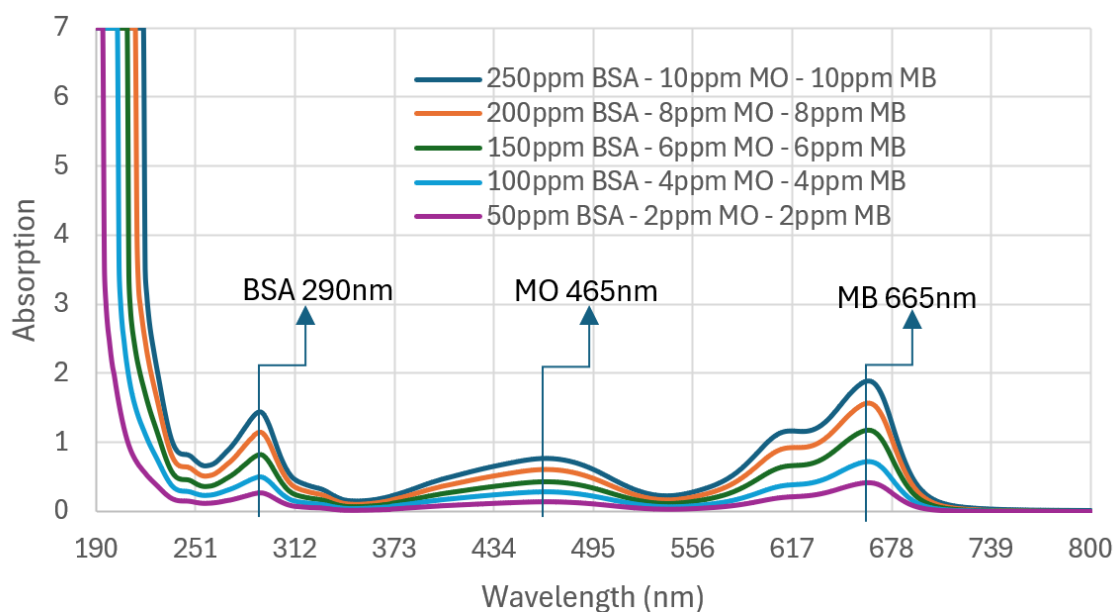


Figure 2: Spectral analysis of different concentrations for model solution

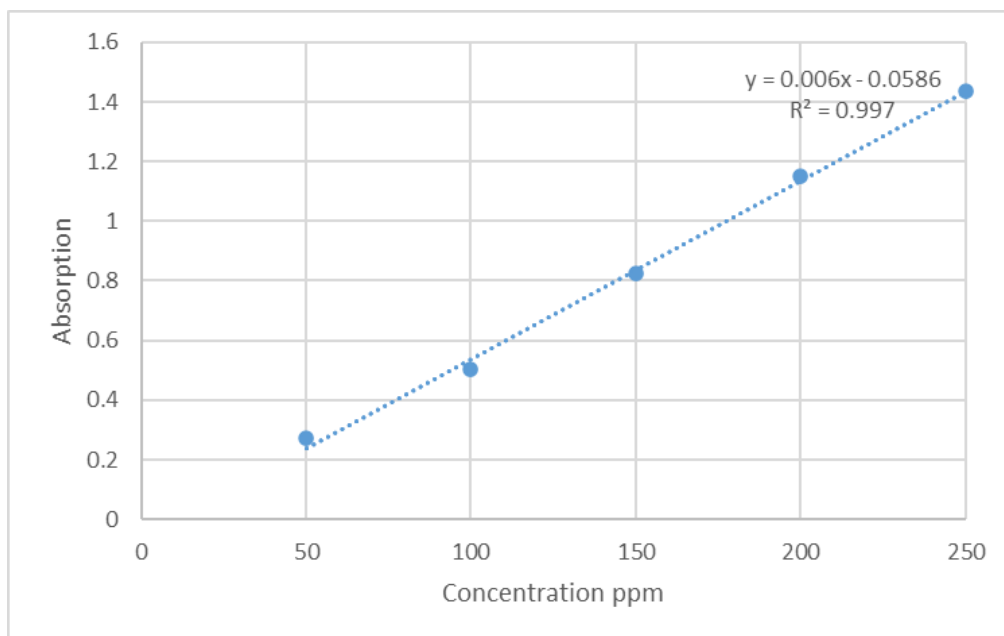


Figure 3: Calibration curve of BSA concentration

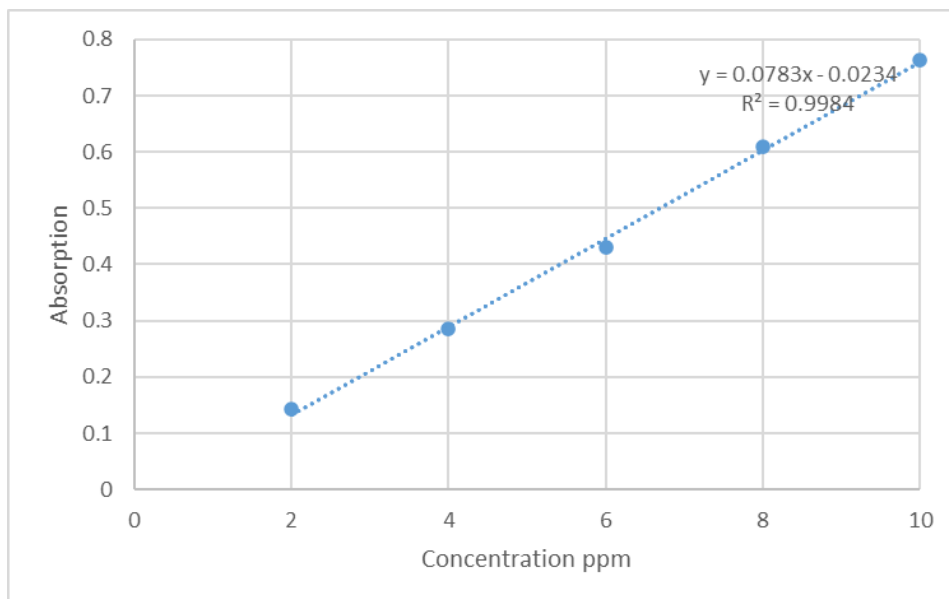


Figure 4: Calibration curve of MO concentration

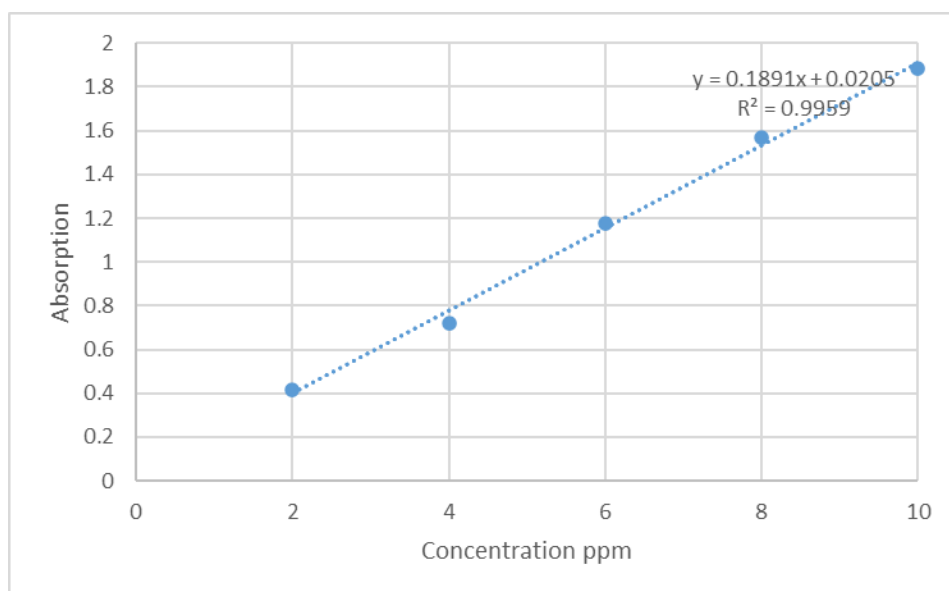


Figure 5: Calibration curve of MB concentration

3.2. Photocatalytic Activity Measurement

The concentrations were calculated in each beaker during the time of the experiment (from 0 till 360 minutes), S1 to S3 represent the different PNPs content (see Table 1). The data shown in Table 2 shows the concentration of BSA, MO and MB for all samples. These concentrations were plotted against the time as shown in Figure 6, Figure 7 and Figure 8 for BSA, MO and MB respectively.

Table 2: Concentrations of BSA, MO and MB in the photocatalytic activity experiment

	Time	BSA			MO			MB		
		S1	S2	S3	S1	S2	S3	S1	S2	S3
Dark	0	250	250	250	10	10	10	10	10	10
	30	247	244	231	9.6	9.6	9.3	9.7	9.7	8.9
	60	247	243	231	9.5	9.3	9.2	9.7	9.6	8.8
	90	247	243	230	9.5	9.3	9.2	9.6	9.6	8.8
	120	230	226	221	3.7	4.3	4.0	9.1	9.0	8.4
Light	150	227	221	211	2.3	2.5	2.3	8.7	8.3	8.1
	180	219	217	209	2.2	2.2	2.0	8.1	7.9	7.6
	210	211	210	207	1.8	1.8	1.8	7.5	7.0	7.0
	240	207	207	201	1.7	1.7	1.7	6.8	6.4	6.3
	300	201	200	198	1.7	1.7	1.6	6.0	5.9	5.6
	330	196	192	191	1.6	1.6	1.5	5.5	5.3	5.0
	360	186	186	182	1.6	1.6	1.5	5.0	4.9	4.4

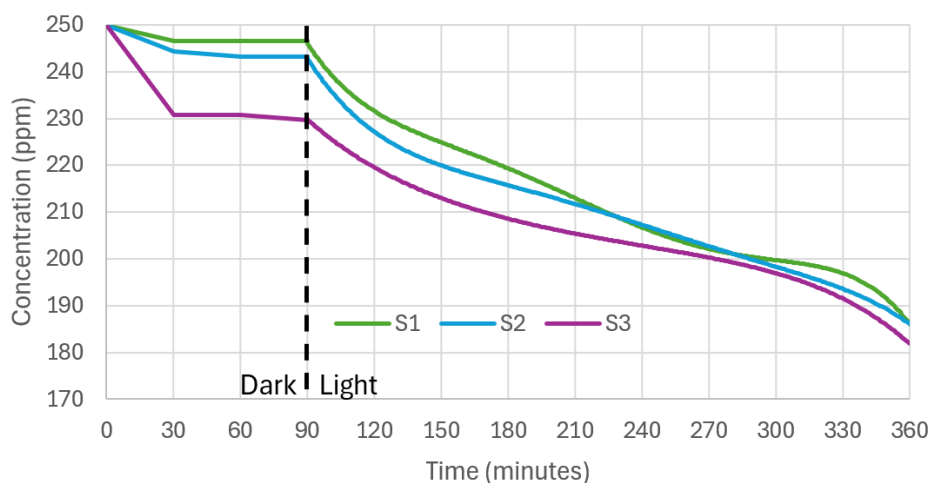


Figure 6: Concentrations of BSA in the photocatalytic activity experiment

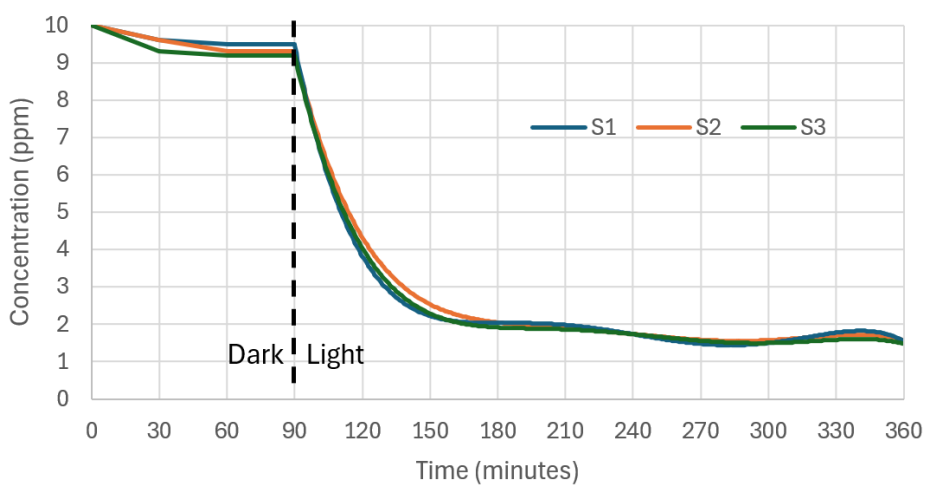


Figure 7: Concentrations of MO in the photocatalytic activity experiment

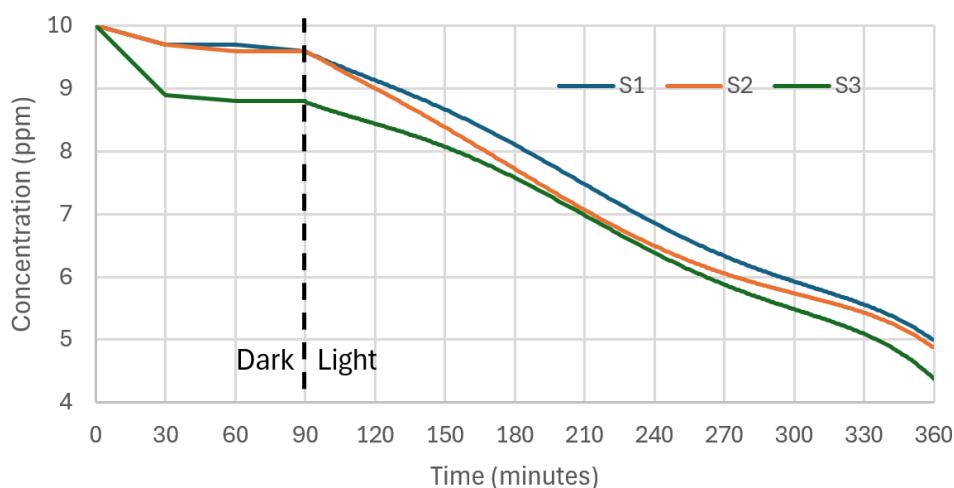


Figure 8: Concentrations of MB in the photocatalytic activity experiment

As shown in the acquired data, during the dark condition, the concentrations of all the substances decrease due to adsorption by membrane material. It was noticed that the adsorption increased with the increase of the PNP content in the membrane, which is due to the nanoparticles increasing the overall capacity of the membrane to capture pollutants from the solution by affecting the membranes' surface charge and porosity providing more active sites for adsorption ¹⁴.

When analyzing the data after subjecting the samples to solar irradiation, the concentrations of the substances are greatly reduced during time, reaching a reduction of 27%, 85%, and 56% to the initial concentrations of BSA, MO and MB respectively during the whole time of the experiment, which represent the substances photodegradation overtime by the PNPs incorporated membranes.

When analyzing the data of S1, S2, and S3 in comparison with each other, which takes into account the boosted photodegradation by the increasing dosage of incorporated PNPs, we find an increase of substance concentration degradation as the percentage of PNPs in the membrane increases.

For BSA, the reactive species generated by PNPs can break down the peptide bonds in BSA, leading to its degradation ⁸. Also, light induces structural changes and denaturation, leading to unfolding and aggregation of the protein. The concentration reduction by photodegradation of BSA represents the least reduction in our study, given that BSA isn't inherently photodegradable, making its denaturation by photocatalytic activity relatively limited ¹⁵.

MO is an azo dye that can be effectively photodegraded under irradiation. This is because MO has an azo bond (-N=N-), which is less stable and more prone to cleavage by reactive species generated during irradiation ¹⁶. This contributes to the high efficiency of the photocatalytic membrane in the photodegradation of MO.

On the other hand, the incorporated PNPs enhance the photodegradation of MB by a substantial value but relatively lower than MO. Unlike MO, MB has a thiazine structure, which includes a sulfur and nitrogen-containing heterocyclic ring. This structure is quite different from the azo bond (-N=N-) found in MO. Having a stronger molecular structure due to its conjugated double bond system, MB shows greater stability and rigidity. The extended conjugation in MB allows for more delocalized electrons, enhancing its stability and making it more resistant to degradation ^{17,18}. Even with lower reduction values than MO, the PNPs still contributed to a prominent influence on the photodegradation of MB ^{19,20}.

For this study, the effect of the PNPs is substantial, relatively to the very small dosage of the PNPs used in the samples, which ranged from 2 to 6 mg in the membrane sample used in the experiment, showing how promising the PNPs used in our study can be utilized in different photocatalytic membrane application. The small percentage of PNPs in our study which ranged from 0.5 to 1.5% weight ratio is more likely to sustain self-cleaning properties for the membrane, providing a prominent antifouling effect without the influence of cleaning chemicals that cut down membrane lifetime. Higher percentages of PNPs would possibly contribute to higher percentages of TrOCs removal.

Further studies should implement other TrOCs for determining the consistency of its behavior, also there can be much improvement to the attained removal efficiency when this technology is combined with activated sludge processes through a photocatalytic membrane bioreactor setup, widening the scope of research in this matter.

4. Conclusion

This research highlights the effectiveness of Ag/TiO₂ nanoparticle-incorporated PES membranes for the photodegradation of TrOCs under simulated sunlight. The study found that the addition of nanoparticles to PES membranes significantly increased the photodegradation rates of BSA, MO and MB. with the highest nanoparticle content yielding the best results. The silver doped TiO₂ revealed its capability of successful photocatalytic activity under visible irradiation. The model solution used emphasizes the fact that the used membrane can efficiently remove TrOCs from wastewater.

These findings suggest that the used nanoparticle-incorporated PES membranes in this study are a viable and scalable solution for advanced water treatment, capable of addressing the limitations of traditional methods and contributing to the sustainable management of water resources.

References

- [1] Subramaniam, M. N. *et al.* Photocatalytic membranes: a new perspective for persistent organic pollutants removal. *Environmental Science and Pollution Research* 2021 29:9 **29**, 12506–12530 (2021).
- [2] Náfrádi, M., Veréb, G., Firak, D. S. & Alapi, T. Photocatalysis: Introduction, Mechanism, and Effective Parameters. 3–31 (2022) doi:10.1007/978-3-030-77371-7_1.
- [3] Davies, K. R., Jones, B., Terashima, C., Fujishima, A. & Pitchaimuthu, S. Photocatalytic Water Pollutant Treatment: Fundamental, Analysis and Benchmarking. *Nanostructured Materials for Environmental Applications* 407–438 (2021) doi:10.1007/978-3-030-72076-6_16/FIGURES/10.
- [4] Koe, W. S., Lee, J. W., Chong, W. C., Pang, Y. L. & Sim, L. C. An overview of photocatalytic degradation: photocatalysts, mechanisms, and development of photocatalytic membrane. *Environmental Science and Pollution Research* 2019 27:3 **27**, 2522–2565 (2019).
- [5] Ayode Otitoju, T., Latif Ahmad, A. & Seng Ooi, B. Recent advances in hydrophilic modification and performance of polyethersulfone (PES) membrane via additive blending. (2018) doi:10.1039/c8ra03296c.
- [6] Abu-Dalo, M. A. *et al.* Photocatalytic Degradation of Methylene Blue Using Polymeric Membranes Based on Cellulose Acetate Impregnated with ZnO Nanostructures. *Polymers* 2021, Vol. 13, Page 3451 **13**, 3451 (2021).
- [7] Wang, J., Pi, H., Zhao, P. & Zhou, N. Efficient removal of methyl orange and ciprofloxacin by reusable Eu–TiO₂ /PVDF membranes with adsorption and photocatalysis methods. *RSC Adv* **14**, 18432–18443 (2024).
- [8] Chakhtouna, H., Benzeid, H., Zari, N., Quaiss, A. el kacem & Bouhfid, R. Recent progress on Ag/TiO₂ photocatalysts: photocatalytic and bactericidal behaviors. *Environmental Science and Pollution Research* 2021 28:33 **28**, 44638–44666 (2021).
- [9] Alenazi, N. A., Hussein, M. A., Alamry, K. A. & Asiri, A. M. Modified polyether-sulfone membrane: A mini review. *Des Monomers Polym* **20**, 532–546 (2017).
- [10] Hui, T. S. & Zaini, M. A. A. Isotherm studies of methylene blue adsorption onto potassium salts-modified textile sludge. *J Teknol* **74**, 57–63 (2015).

- [11] Razali, N. A. *et al.* Preliminary screening oxidative degradation methyl orange using ozone/ persulfate. *E3S Web of Conferences* **34**, (2018).
- [12] Boopathy, G., Gangasalam, A. & Mahalingam, A. Photocatalytic removal of organic pollutants and self-cleaning performance of PES membrane incorporated sulfonated graphene oxide/ZnO nanocomposite. *Journal of Chemical Technology and Biotechnology* **95**, 3012–3023 (2020).
- [13] 13.HOWELL JA & BOLTZ DF. Spectrophotometry and Spectrofluorimetry: A Practical Approach. *Modern Analytical Techniques for Metals and Alloys, Tech of Metals Res* **3**, 225–274 (2000).
- [14] Gao, J. *et al.* Enhanced effect of adsorption and photocatalysis by TiO₂ nanoparticles embedded porous PVDF nanofiber scaffolds. *J Mater Res* **36**, 1538–1548 (2021).
- [15] Matsarskaia, O. *et al.* Evolution of the structure and dynamics of bovine serum albumin induced by thermal denaturation. *Physical Chemistry Chemical Physics* **22**, 18507–18517 (2020).
- [16] Regraguy, B. *et al.* Photocatalytic degradation of methyl orange in the presence of nanoparticles NiSO₄/TiO₂. *Nanotechnology for Environmental Engineering* **7**, 157–171 (2022).
- [17] Canossa, S., Graiff, C., Crocco, D. & Predieri, G. Water Structures and Packing Efficiency in Methylene Blue Cyanometallate Salts. *Crystals 2020, Vol. 10, Page 558* **10**, 558 (2020).
- [18] Madduri, S. B. & Kommalapati, R. R. Photocatalytic Degradation of Azo Dyes in Aqueous Solution Using TiO₂ Doped with rGO/CdS under UV Irradiation. *Processes* **12**, 1455 (2024).
- [19] Sonu, K., Puttaiah, S. H., Raghavan, V. S. & Gorthi, S. S. Photocatalytic degradation of MB by TiO₂: studies on recycle and reuse of photocatalyst and treated water for seed germination. *Environmental Science and Pollution Research* **28**, 48742–48753 (2021).
- [20] Brik, A. *et al.* Photodegradation of methylene blue under UV and visible light irradiation by Er₂O₃-coated silicon nanowires as photocatalyst. *Reaction Kinetics, Mechanisms and Catalysis* **131**, 525–536 (2020).

Supplementary Information Not Applicable

Declarations

Funding: The authors have not received any funding concerning this article.

Competing interests: There are no competing interests in this study.

Ethics approval and consent to participate: In this specific research project, it does not apply since it is not considered that there are ethical conflicts.

Consent to participate All authors consent to participate in the research project.

Consent for publication All authors consent to publish the article in question.

Availability of data and material: Enquiries about data availability should be directed to the authors

Hussein Mahmoud El-Ghorab	husseinelghorab@eng.asu.edu.eg
Mahmoud Mohamed Abdel Azeem	mazeem@eng.asu.edu.eg
Mohamed Ismail Badawy	badawy46@hotmail.com
Tarek Abdel Shafy Gad Allah	tareqabdelshafy@yahoo.ca
Mahmoud Saad Abdel Wahed	ms.abdel-wahed@nrc.sci.eg
Mahmoud Mohamed Abdelmomen	mahmoud_abdelmomen@eng.asu.edu.eg

Authors' contributions:

- HM (Hussein Mahmoud El-Ghorab): participate by 30% by data collection and writing the manuscript.
- MMA (Mahmoud Mohamed Abdel Azeem): participate by 5% by co-suggesting the research idea, and the general supervision.
- MI (Mohamed Ismail Badawy): participate by 5% by co-suggesting the research idea, and the general supervision.
- TA (Tarek Abdel Shafy Gad Allah): participate by 20% by deciding the article structure and revising this manuscript.
- MS (Mahmoud Saad Abdel Wahed): participate by 20% by aid in writing and editing of the manuscript.
- MMM (Mahmoud Mohamed Abdelmomen): participate by 20% by aid in writing and editing of the manuscript.
- All authors read and approved the final manuscript.